Three-photon Stokes-Mueller polarimetry

Masood Samim, Serguei Krouglov, and Virginijus Barzda*
Department of Chemical and Physical Sciences, Department of Physics and Institute for Optical Sciences, University of Toronto, 3359 Mississauga Road North, Mississauga, Ontario, Canada L5L1C6
(Received 21 December 2015; revised manuscript received 29 January 2016; published 22 March 2016)

The generalized theory of Stokes-Mueller polarimetry is employed to develop the third-order optical polarimetry framework for third-harmonic generation (THG). The outgoing and incoming radiations are represented by 4-element and 16-element column vectors, respectively, and the intervening medium is represented by a 4×16 triple Mueller matrix. Expressions for the THG Stokes vector and the Mueller matrix are provided in terms of coherency and correlation matrices and expanded by four-dimensional γ matrices that are analogs of Pauli matrices. Useful expressions of triple Mueller matrices are presented for cylindrically symmetric and isotropic structures. In addition, the relation between third-order susceptibilities and the measured triple Mueller matrix is provided. This theoretical framework can be applied for structural investigations of crystalline materials, including biological structures.

DOI: 10.1103/PhysRevA.93.033839

I. INTRODUCTION

Three-photon processes such as third-harmonic generation (THG) reveal unique structural information about the sample under study [1–4]. The generated third-harmonic signal from the material is related to the incoming radiation electric fields and determined by the third-order susceptibility tensor $\chi^{(3)}$ of the material [2]. The third-harmonic generation is an odd order process and has markedly different symmetry selection rules compared to the even order processes.

Stokes-Mueller, Poincaré, or Jones formalism can be used to describe the polarization dependence of the interaction of light with a medium, each approach having its unique advantage [5–7]. The Stokes-Mueller method can account for unpolarized light and describes the depolarization process. The light polarization in the context of Stokes-Mueller formalism is represented by a vector, and the interaction of the radiation with matter is denoted by a matrix. Both partially or completely polarized light can be represented by the Stokes vector, which contains real-valued components and is composed of light intensities that can be measured in an experiment.

The nonlinear Stokes-Mueller equation for the third-order processes describes the relationship between the generated nonlinear signal radiation, the nonlinear properties of the media, and the incoming radiations:

$$s'(\omega_\sigma) = \mathcal{M}^{(3)} S^{(3)}(\omega_1,\omega_2,\omega_3) \quad (1)$$

where s' is the conventional 4×1 Stokes vector of the generated radiation at ω_σ frequency and prime signifies the measured outgoing signal, while $S^{(3)}$ is a 16×1 triple Stokes vector representing the polarization state of the three incoming electric fields (with frequencies ω_1, ω_2, and ω_3) that generate the light via nonlinear interactions. For THG the incoming radiation frequencies are all the same (Fig. 1). Henceforth, the s' and $S^{(3)}$ are called the polarization state vectors for outgoing and incoming radiations, respectively. The triple Mueller matrix $\mathcal{M}^{(3)}$ describes the material properties of a third-order light-matter interaction. The Mueller matrix contains the nonlinear susceptibilities, which are independent of the incoming radiation intensities. The nonlinear Stokes-Mueller polarimetry is applicable for nonionizing radiations in the optical range (i.e. $I_{\text{laser}} \ll I_{\text{atomic}} = 4 \times 10^{20}\ \text{W/m}^2$), and the intensity independence of the Mueller matrix components can be tested by performing polarimetry measurements with several incoming radiation intensities [2,8].

In this paper, we concentrate on the three-photon processes, and develop specific equations for the THG from the generalized Stokes-Mueller polarimetry formalism [8]. The derivation will follow the same formalism that we used for the second-harmonic generation process as well as the generalization for other nonlinear optical processes [8,9]. In Sec. II we will develop the equations for the outgoing and incoming radiation polarization states, followed by the expression for the triple Mueller matrix in Sec. III. Specific examples of the Mueller matrix for real-valued susceptibilities with isotropic and hexagonal symmetries will be provided, which have relevance to biological structures. The formalism introduced in this paper is applicable for measurements in thin samples, i.e., the phase matching conditions and diffraction of waves for nonplanar samples is not considered. The THG signal has been previously observed from thin samples such as β-carotene microcrystals in orange carrot, retinal in membranes of fruit fly eye, astaxanthin aggregates in green algae, and melanin in melanoma cells [1,10–17]. The method for extracting susceptibility component values from the Mueller matrix will be provided in Sec. IV. The expressions for the triple Stokes-Mueller polarimetric measurements will be presented in Sec. V, including equations for the reduced polarimetry with linear polarization states of incoming and outgoing radiations.

II. DERIVATION OF POLARIZATION STATE OF RADIATIONS

A. Outgoing radiation Stokes vector

The Stokes vector s' for the outgoing third-harmonic radiation is characterized by a 4×1 vector just as in the case for the conventional Stokes vector. The coherency matrix of

*virgis.barzda@utoronto.ca

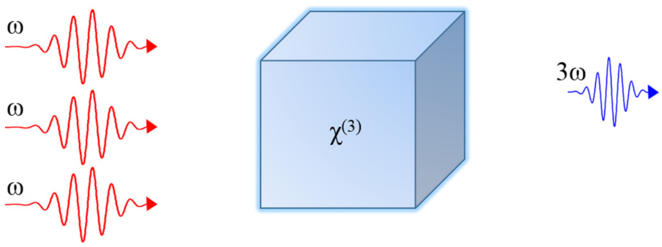

FIG. 1. Schematic representation of a third-harmonic generation process analyzed by polarimetry. Three photons of incoming beam with frequency ω are incident onto the sample possessing the third-order susceptibility $\chi^{(3)}$, and the emitted radiation is at thrice the incoming frequency, 3ω. In three-photon polarimetry, the incoming radiation is represented by the triple Stokes vector $S^{(3)}$, the medium is characterized with the matrix $\mathcal{M}^{(3)}$, and the outgoing measured signal is represented by a 4×1 Stokes vector s'.

the third-harmonic signal is [7,8]

$$C'_{ab}(3\omega) = \langle \Phi'(3\omega) \cdot \Phi'^{\dagger}(3\omega)\rangle_{ab} = \langle \Phi'_a(3\omega)\Phi'^{*}_b(3\omega)\rangle \quad (2)$$

where a and b each run from 1 to 2, representing the orthogonal outgoing polarization orientations perpendicular to the light propagation direction, and $\Phi'(3\omega)$, which is directly proportional to the polarization density $P^{(3)}$, is the state (or simply the electric-field) vector of the outgoing beam. The dagger symbol $\dagger$ denotes the complex conjugation and transposition. $\langle\cdot\rangle$ signifies a time average over an interval long enough to make the time averaging independent of the interval and fluctuations. Then, the outgoing radiation Stokes vector is [7–9]

$$s'_t = \mathrm{Tr}(C'\tau_t) = C'_{ab}(\tau_t)_{ba} = \langle \Phi'_a \Phi'^{*}_b\rangle(\tau_t)_{ba} = \langle \Phi'^{\dagger}\tau_t\Phi'\rangle \quad (3)$$

where τ_t ($t = 0...3$) denotes the 2×2 identity and Pauli matrices, which are Hermitian and obey the unique orthogonality relation $\mathrm{Tr}(\tau_\mu\tau_\nu) = 2\delta_{\mu\nu}$, where $\delta_{\mu\nu}$ is the Kronecker delta (see Appendix A). Additionally, the degree of polarization ($0 \leqslant \mathscr{P}' \leqslant 1$) of the outgoing radiation in terms of its Stokes vector components can be obtained according to [18]

$$\mathscr{P}' = \sqrt{{s'_1}^2 + {s'_2}^2 + {s'_3}^2}/s'_0. \quad (4)$$

The degree of polarization $\mathscr{P}'$ provides information about the scattering and depolarization of the third-harmonic radiation.

B. Real-valued triple Stokes vector

The third-order nonlinear signal is generated due to induced nonlinear polarization $P_i^{(3)}$ in the material:

$$P_i^{(3)} = \chi^{(3)}_{ijkl}E_jE_kE_l = \chi^{(3)}_{iA}\psi^{(3)}_A \quad (5)$$

where the first index i indicates the direction of outgoing polarization, while the indices j, k, and l indicate the direction of polarization of incoming electric fields, and summation is assumed over the repeated indices [2,8]. The index A is composed of the indices j,k,l and depends on the third-order process being studied (i.e., THG, coherent anti-Stokes Raman scattering (CARS), etc.).

For triple Stoke-Mueller polarimetry of THG, the incoming radiation electric-field state vector $\psi^{(3)}(\omega_1,\omega_2,\omega_3)$ has the same frequency ω for all three electric fields. Therefore the polarization state is

$$\psi^{(3)}(\omega,\omega,\omega) = \begin{pmatrix} {E_1}^3 \\ {E_2}^3 \\ 3{E_1}^2E_2 \\ 3E_1{E_2}^2 \end{pmatrix} \quad (6)$$

where the subscripts 1 and 2 represent the orthogonal electric-field vector orientations forming the plane perpendicular to the light propagation. Thus, the coherency matrix for the three-photon process is

$$\rho^{(3)}(\omega,\omega,\omega) = \langle\psi^{(3)}\cdot\psi^{(3)\dagger}\rangle = \begin{pmatrix} \langle {E_1}^3 E_1^{*3}\rangle & \langle {E_1}^3 E_2^{*3}\rangle & \langle 3\,{E_1}^3 E_1^{*2}E_2^*\rangle & \langle 3\,{E_1}^3 E_1^{*}E_2^{*2}\rangle \\ \langle {E_2}^3 E_1^{*3}\rangle & \langle {E_2}^3 E_2^{*3}\rangle & \langle 3\,{E_2}^3 E_1^{*2}E_2^*\rangle & \langle 3\,{E_2}^3 E_1^{*}E_2^{*2}\rangle \\ \langle 3\,{E_1}^2E_2 E_1^{*3}\rangle & \langle 3\,{E_1}^2E_2 E_2^{*3}\rangle & \langle 9\,{E_1}^2E_2 E_1^{*2}E_2^*\rangle & \langle 9\,{E_1}^2E_2 E_1^{*}E_2^{*2}\rangle \\ \langle 3\,E_1{E_2}^2 E_1^{*3}\rangle & \langle 3\,E_1{E_2}^2 E_2^{*3}\rangle & \langle 9\,E_1{E_2}^2 E_1^{*2}E_2^*\rangle & \langle 9\,E_1{E_2}^2 E_1^{*}E_2^{*2}\rangle \end{pmatrix}$$

$$= \begin{pmatrix} C_{11}^3 & C_{12}^3 & 3\,C_{11}^2\,C_{12} & 3\,C_{11}\,C_{12}^2 \\ C_{21}^3 & C_{22}^3 & 3\,C_{21}^2\,C_{22} & 3\,C_{21}\,C_{22}^2 \\ 3\,C_{11}^2\,C_{21} & 3\,C_{12}^2\,C_{22} & 9\,C_{11}^2\,C_{22} & 9\,C_{12}^2\,C_{21} \\ 3\,C_{11}\,C_{21}^2 & 3\,C_{12}\,C_{22}^2 & 9\,C_{12}\,C_{21}^2 & 9\,C_{11}\,C_{22}^2 \end{pmatrix} \quad (7)$$

where C is the ordinary 2×2 coherency matrix for the fundamental beam with frequency ω [18]. In Eq. (7), going from the first to the second matrix, we assume $\langle E_jE_kE_lE_m^*E_n^*E_o^*\rangle = \langle E_jE_m^*\rangle\langle E_kE_n^*\rangle\langle E_lE_o^*\rangle$ (indices j,k,l,m,n, and o each run from 1 to 2), which allows us to use the conventional coherency matrix to redefine the interacting electric fields. This assumption is justified if the incident radiation is coherent and fully polarized, i.e., from a laser source. Note that the requirement for a coherent and polarized light source is given for nonlinear optical processes, because the noncoherent fundamental radiation is not expected to generate a significant THG signal. Furthermore, this assumption simplifies other equations derived later.

The general triple Stokes vector can be found similar to the linear and two-photon processes according to

$$S_N^{(3)}(3\omega) = \mathrm{Tr}\big(\rho^{(3)}\,\gamma_{_N}\big) = \big\langle \psi_A^{(3)}\psi_B^{(3)*}\big\rangle (\gamma_{_N})_{BA} \tag{8}$$

where A and $B = 1,\ldots,4$, $N = 1,\ldots,16$, and the 4×4 γ matrices and the associated identity matrix are analogous to Pauli matrices. They are Hermitian and obey the unique orthogonality relation $\mathrm{Tr}(\gamma_M\gamma_N) = 2\delta_{MN}$ (see Appendix A). Therefore, the elements of the triple Stokes vector describing the polarization state for incoming radiation are

$$S_N^{(3)}(\omega,\omega,\omega) = \begin{pmatrix} \frac{\sqrt{2}}{2}\big(\langle E_1{}^3\,E_1^{*3}\rangle + \langle 9E_1{}^2\,E_2\,E_1^{*2}\,E_2^{*}\rangle + \langle 9E_1\,E_2{}^2\,E_1^{*}\,E_2^{*2}\rangle + \langle E_2{}^3\,E_2^{*3}\rangle\big)\\ \frac{\sqrt{6}}{6}\big(\langle E_1{}^3\,E_1^{*3}\rangle + \langle 9E_1{}^2\,E_2\,E_1^{*2}\,E_2^{*}\rangle - \langle 27E_1\,E_2{}^2\,E_1^{*}\,E_2^{*2}\rangle + \langle E_2{}^3\,E_2^{*3}\rangle\big)\\ \frac{\sqrt{3}}{3}\big(\langle E_1{}^3\,E_1^{*3}\rangle - \langle 18E_1{}^2\,E_2\,E_1^{*2}\,E_2^{*}\rangle + \langle E_2{}^3\,E_2^{*3}\rangle\big)\\ \langle E_1{}^3\,E_1^{*3}\rangle - \langle E_2{}^3\,E_2^{*3}\rangle\\ \langle E_1{}^3\,E_2^{*3}\rangle + \langle E_2{}^3\,E_1^{*3}\rangle\\ \langle 3\,E_1{}^2\,E_2\,E_2^{*3}\rangle + \langle 3\,E_2{}^3\,E_1^{*2}\,E_2^{*}\rangle\\ \langle 9\,E_1{}^2\,E_2\,E_1^{*}\,E_2^{*2}\rangle + \langle 9\,E_1\,E_2{}^2\,E_1^{*2}\,E_2^{*}\rangle\\ \langle 3\,E_1^{*}\,E_2{}^3\,E_2^{*2}\rangle + \langle 3\,E_1\,E_2{}^2\,E_2^{*3}\rangle\\ \langle 3\,E_2^{*}\,E_1{}^3\,E_1^{*2}\rangle + \langle 3\,E_2\,E_1{}^2\,E_1^{*3}\rangle\\ \langle 3\,E_1{}^3\,E_1^{*}\,E_2^{*2}\rangle + \langle 3\,E_1\,E_2{}^2\,E_1^{*3}\rangle\\ \big(\langle E_1{}^3\,E_2^{*3}\rangle - \langle E_2{}^3\,E_1^{*3}\rangle\big)\mathrm{i}\\ \big(\langle 3\,E_2{}^3\,E_1^{*2}\,E_2^{*}\rangle - \langle 3\,E_1{}^2\,E_2\,E_2^{*3}\rangle\big)\mathrm{i}\\ \big(\langle 9\,E_1{}^2\,E_2\,E_1^{*}\,E_2^{*2}\rangle - \langle 9\,E_1\,E_2{}^2\,E_1^{*2}\,E_2^{*}\rangle\big)\mathrm{i}\\ \big(\langle 3\,E_2{}^3\,E_1^{*}\,E_2^{*2}\rangle - \langle 3\,E_1\,E_2{}^2\,E_2^{*3}\rangle\big)\mathrm{i}\\ \big(\langle 3\,E_1{}^3\,E_1^{*2}\,E_2^{*}\rangle - \langle 3\,E_1{}^2\,E_2\,E_1^{*3}\rangle\big)\mathrm{i}\\ \big(\langle 3\,E_1{}^3\,E_1^{*}\,E_2^{*2}\rangle - \langle 3\,E_1\,E_2{}^2\,E_1^{*3}\rangle\big)\mathrm{i} \end{pmatrix} = \frac{1}{4}\begin{pmatrix} \sqrt{2}s_0\big(5s_0{}^2 - 3s_1{}^2\big)\\ \sqrt{6}\big(-\frac{4}{3}s_0{}^3 + 3\,s_0{}^2\,s_1 + 2\,s_0\,s_1{}^2 - 3\,s_1{}^3\big)\\ \sqrt{3}\big(-\frac{8}{3}s_0{}^3 - 3\,s_0{}^2\,s_1 + 4\,s_0\,s_1{}^2 + 3\,s_1{}^3\big)\\ s_1\big(3\,s_0{}^2 + s_1{}^2\big)\\ s_2\big(s_2{}^2 - 3\,s_3{}^2\big)\\ 3(s_0 - s_1)\big(s_2{}^2 - s_3{}^2\big)\\ 9s_2\big(s_2{}^2 + s_3{}^2\big)\\ 3\,s_2\,(s_0 - s_1)^2\\ 3\,s_2\,(s_0 + s_1)^2\\ 3(s_0 + s_1)\big(s_2{}^2 - s_3{}^2\big)\\ s_3\big(3\,s_2{}^2 - s_3{}^2\big)\\ -6s_2\,s_3\,(s_0 - s_1)\\ 9s_3(s_2{}^2 + s_3{}^2)\\ -3s_3\,(s_0 - s_1)^2\\ 3s_3\,(s_0 + s_1)^2\\ 6s_2\,s_3\,(s_0 + s_1) \end{pmatrix} \tag{9}$$

where s_0, s_1, s_2, and s_3 are the Stokes vector components of incoming laser polarization (note that here and throughout the paper $\mathrm{i} = \sqrt{-1}$ denotes the imaginary number, while i denotes an index). The second equality of Eq. (9) is valid for fully coherent and polarized states of the incoming laser radiation. For a partially polarized fundamental radiation the incoherent part is not expected to contribute significantly to the nonlinear signal. Therefore for the analysis of experimental results with partially polarized beam, s_0 of the fundamental laser beam can be calculated as $s_0^2 = s_1^2 + s_2^2 + s_3^2$ and used for the triple Stokes vector in the Stokes-Mueller polarimetry Eqs. (7) and (9). Note, the last six elements of the vector above vanish when s_3 is zero. It implies that the triple Stokes vector for THG will have at most the first ten nonzero elements if the incoming radiation is linearly polarized.

Additionally, the first element S_1 is proportional to the trace of the coherency matrix in Eq. (7), which is proportional to the electric fields and the intensity of the incoming radiation. In fact, the vector for third-order interaction obeys the following relation [8]:

$$3S_1^2 \geqslant \sum_{N=2}^{16} S_N^2 \tag{10}$$

where the equality is valid for a purely polarized state. Therefore, it is convenient to use the degree of polarization $\mathscr{P}^{(3)}$ parameter to characterize the fundamental radiation:

$$\mathscr{P}^{(3)}(\omega,\omega,\omega) = \sqrt{\sum_{N=2}^{16} S_N^2/3S_1^2} \tag{11}$$

where $\mathscr{P}^{(3)}$ ranges from zero to one, which may denote the unpolarized to fully polarized fundamental radiation, respectively. Note that the definition of the degree of polarization for multiple interacting fields is not necessarily unique. The conventional degree of polarization is unique only for the two-field case, whereas for the three-field case there are at least three different ways to define the degree of polarization. The definition of $\mathscr{P}^{(3)}$ in Eq. (11) by analogy is similar to the conventional form of the degree of polarization for two electric fields and, as has been previously suggested, is more convenient than other definitions [19,20].

III. INTERVENING MEDIUM: TRIPLE MUELLER MATRIX $\mathcal{M}^{(3)}$

By substituting linear and nonlinear Stokes vector expressions [Eqs. (3) and (8), respectively] into the general nonlinear polarimetry Eq. (1) the following expression is obtained:

$$\langle \Phi'^{\dagger}\, \tau_t\, \Phi' \rangle = \mathcal{M}^{(3)}_{tN} \langle \psi^{(3)\dagger}\, \gamma_{N}\, \psi^{(3)} \rangle. \tag{12}$$

In this framework, each component of the vector Φ' of the generated electric field is proportional to the polarization state of incoming electric field and to the susceptibility tensor components of the material. By substituting explicit expressions of Φ' and $\Phi'^{\dagger}$ into Eq. (12) in the elemental form the following equation is obtained:

$$\left\langle \chi^{(3)*}_{aA} \psi^{*}_{A} (\tau_t)_{ab} \chi^{(3)}_{bB} \psi_B \right\rangle = \mathcal{M}^{(3)}_{tN} \left\langle \psi^{(3)*}_{A} \left(\gamma_{N}\right)_{AB} \psi^{(3)}_{B} \right\rangle \tag{13}$$

where the contracted notation A and $B = 1,\ldots,4$ in $\chi^{(3)}_{iA} = \chi^{(3)}_{ijkl}$ is defined as

$$\begin{array}{lcccc} jkl: & 111 & 222 & 112,121,211 & 122,212,221 \\ A: & 1 & 2 & 3 & 4 \end{array} \tag{14}$$

and the same contracted notation is used for B. Note that here the matrix is constructed mainly with the THG process in mind, where the Kleinman symmetry is not required. In comparison to the linear Mueller matrix elements, which are composed of products of linear susceptibilities and Pauli matrices, the triple $\mathcal{M}^{(3)}$ is composed of nonlinear susceptibilities and 4×4 γ matrices. In addition, similar to the linear polarimetry, all elements of the matrix for the nonlinear interaction are real; this conclusion leads to a very useful and desired expression for obtaining the nonlinear susceptibilities as will be shown in Sec. IV. In extending the matrix for other third-order processes it may be required to ensure that the Kleinman symmetry is valid. Otherwise, an effective $\chi^{(3)}$ is defined, or the dimensions of the γ matrices must be increased.

In a highly scattering media such as biological tissue, the system may not be completely coherent, and the source of the signal may be an ensemble of scatterers. Therefore, an ensemble average of individual elements with probability p_e may be more appropriate to consider [21]. In addition, since Eq. (13) is written in terms of individual elements, the state functions of the fundamental radiation can be dropped and the nonlinear Mueller matrix elements $\mathcal{M}_{tN}$ can be written in terms of the third-order susceptibilities as

$$\mathcal{M}^{(3)}_{tN} = \tfrac{1}{2}\left[\sum_{e} p_e \left(\chi^{(3,e)*}_{aA} \chi^{(3,e)}_{bB}\right)\right] (\tau_t)_{ab} (\gamma_{N})_{BA} \tag{15}$$

where summation is assumed over repeated indices. In deriving Eq. (15) for the ensemble of $\chi^{(3)}$ the order of variables is a nonissue because both equations [Eqs. (13) and (15)] are expressed in the elemental form. The correlation matrix contains information about the ensemble, and in the case of a homogeneous medium reduces to a product of $\chi^{(3)*}_{aA}\chi^{(3)}_{bB}$ of a single source.

Note that the outgoing radiation may not be fully polarized, since the generated light is no longer originating from a single source, but rather from an ensemble of sources. Thus, Eq. (15) is a better representation of experimental data from a heterogeneous medium.

Similar to the symbolic notation that was given for the second-order matrix $\mathcal{M}^{(2)}$ (see Ref. [9]), the symbolic matrix for the third-order $\mathcal{M}^{(3)}$ becomes

$$\begin{pmatrix} NP & NP & NP & NP & I^c_{\diamond} & I^c_{\Delta} & I^c_{\nabla} & I^c_{\triangleleft} & I^c_{\triangleright} & I^c_{\square} & I^s_{\diamond} & I^s_{\Delta} & I^s_{\nabla} & I^s_{\triangleleft} & I^s_{\triangleright} & I^s_{\square} \\ NP & NP & NP & NP & I^c_{\diamond} & I^c_{\Delta} & I^c_{\nabla} & I^c_{\triangleleft} & I^c_{\triangleright} & I^c_{\square} & I^s_{\diamond} & I^s_{\Delta} & I^s_{\nabla} & I^s_{\triangleleft} & I^s_{\triangleright} & I^s_{\square} \\ O^c & O^c & O^c & O^c & OI^c_{\diamond} & OI^c_{\Delta} & OI^c_{\nabla} & OI^c_{\triangleleft} & OI^c_{\triangleright} & OI^c_{\square} & OI^s_{\diamond} & OI^s_{\Delta} & OI^s_{\nabla} & OI^s_{\triangleleft} & OI^s_{\triangleright} & OI^s_{\square} \\ O^s & O^s & O^s & O^s & OI^s_{\diamond} & OI^s_{\Delta} & OI^s_{\nabla} & OI^s_{\triangleleft} & OI^s_{\triangleright} & OI^s_{\square} & OI^c_{\diamond} & OI^c_{\Delta} & OI^c_{\nabla} & OI^c_{\triangleleft} & OI^c_{\triangleright} & OI^c_{\square} \end{pmatrix}. \tag{16}$$

The superscripts s and c denote the sin and cos of the relative phase between the susceptibility tensor elements that make up the triple Mueller matrix element. Phase-independent (NP) elements are present in the first two rows and four columns and are composed of the squares of susceptibility components; those dependent on the incoming I index are situated in the first two rows and last twelve columns; elements dependent on the outgoing O index are located in the last two rows and first four columns; and the elements that depend on incoming as well as outgoing OI indices form the remaining elements.

Additionally, the following symmetry features of the triple Mueller matrix can be seen: Columns 5 to 10 of the triple Mueller matrix ($N = 5,\ldots,10$) have the same susceptibility products as columns 11 to 16 ($N + 6$), respectively, where the retardedness of the components in the last six columns acquires an additional $\pi/2$ phase shift relative to the six columns before them (superscripts c and s). The corresponding columns with the same susceptibilities are indicated as subscripts $\diamond$, Δ, ∇, $\triangleleft$, $\triangleright$, and $\square$ in the symbolic matrix (16). In the following, explicit expressions of the triple Mueller matrix for a few special cases will be presented.

Triple Mueller matrix for real susceptibilities

When susceptibilities are real, the Mueller matrix components that have sin dependency on the retardance phase reduce to zero [see the components with superscript s in the symbolic Mueller matrix (16)]. Therefore, the last six columns of the first three rows and the first ten elements of the last row in $\mathcal{M}^{(3)}$ are zero. In addition, if Kleinman symmetry is valid for a third-order process, then there are five unique nonzero susceptibilities. The Mueller matrix can be expressed by using four unique susceptibility component ratios as follows:

$$\mathcal{M}^{(3)}_{\text{THG,Kleinman}} = \left(\chi^{(3)}_{14}\right)^2 \left(\begin{array}{cccccccccccccccc} \frac{\sqrt{2}}{4}(a^2+b^2+2c^2+2d^2+2) & \frac{\sqrt{6}}{12}(a^2+b^2+2c^2-2d^2-2) & \frac{\sqrt{3}}{6}(a^2+b^2-c^2+d^2-2) & (a^2-b^2+c^2-d^2)/2 & ad+bc & cd+b & c+d & d(1+b) & c(a+1) & a+cd & 0 & 0 & 0 & 0 & 0 & 0 \\ \frac{\sqrt{2}}{4}(a^2-b^2) & \frac{\sqrt{6}}{12}(a^2-b^2+4d^2-4) & \frac{\sqrt{3}}{6}(a^2-b^2-3c^2+d^2+2) & (a^2+b^2-c^2-d^2)/2 & ad-bc & cd-b & c-d & d(1-b) & c(a-1) & a-cd & 0 & 0 & 0 & 0 & 0 & 0 \\ \frac{\sqrt{2}}{2}(c+d+ac+bd) & \frac{\sqrt{6}}{6}(c-3d+ac+bd) & \frac{\sqrt{3}}{3}(ac-2c+bd) & ac-bd & ab+cd & d+bc & cd+1 & d^2+b & c^2+a & c+ad & 0 & 0 & 0 & 0 & 0 & 0 \\ 0 & 0 & 0 & 0 & 0 & 0 & 0 & 0 & 0 & 0 & ab-cd & d-bc & cd-1 & d^2-b & a-c^2 & ad-c \end{array}\right) \tag{17}$$

where $a = \chi^{(3)}_{11}/\chi^{(3)}_{14}$, $b = \chi^{(3)}_{22}/\chi^{(3)}_{14}$, $c = \chi^{(3)}_{13}/\chi^{(3)}_{14}$, and $d = \chi^{(3)}_{12}/\chi^{(3)}_{14}$. An interesting prediction is that when the incoming radiations are linearly polarized the outgoing s'_3 will be zero. That occurs because the last six components of the triple Stokes vector are zero for linearly polarized incoming light [see Eq. (9)], and the first ten elements of the last row in $\mathcal{M}^{(3)}$ are zero for real-valued susceptibilities [see Eq. (17)]. The condition of real-valued susceptibilities is further explored in two more specific cases.

1. *Triple Mueller matrix for isotropic media*

For isotropic material with real susceptibilities, only three susceptibility components are nonzero, of which only one is independent: $\chi^{(3)}_{11} = \chi^{(3)}_{22} = 3\chi^{(3)}_{14}$ [2]. By substituting these symmetry relations into Eq. (17), the matrix for isotropic material is obtained as follows:

$$\mathcal{M}^{(3)}_{\text{iso}} = \left(\chi^{(3)}_{14}\right)^2 \begin{pmatrix} 5\sqrt{2} & \frac{4\sqrt{6}}{3} & \frac{8\sqrt{3}}{3} & 0 & 0 & 3 & 0 & 0 & 0 & 3 & 0 & 0 & 0 & 0 & 0 & 0 \\ 0 & -\frac{\sqrt{6}}{3} & \frac{\sqrt{3}}{3} & 9 & 0 & -3 & 0 & 0 & 0 & 3 & 0 & 0 & 0 & 0 & 0 & 0 \\ 0 & 0 & 0 & 0 & 9 & 0 & 1 & 3 & 3 & 0 & 0 & 0 & 0 & 0 & 0 & 0 \\ 0 & 0 & 0 & 0 & 0 & 0 & 0 & 0 & 0 & 0 & 9 & 0 & -1 & -3 & 3 & 0 \end{pmatrix}. \tag{18}$$

As can be seen, and may readily be verified by an experiment, the matrix elements for isotropic material scale only with an effective susceptibility value.

2. *Triple Mueller matrix for hexagonal symmetry*

For materials possessing hexagonal and Kleinman symmetry, three elements are independent: $\chi^{(3)}_{11}$, $\chi^{(3)}_{22}$, and $\chi^{(3)}_{14}$. Substituting them in Eq. (17), the hexagonal material matrix assumes the form expressed in Eq. (19).

Equation (19) assumes that the cylindrical axis is oriented along the axis $i = 1$. The experimentally measured Mueller matrix can be used to extract the susceptibility values of the material. For example, the cylindrically symmetric crystalline aggregates of biologically important molecules such as astaxsanthin and β-carotene have been characterized with THG polarimetric microscopy and $\chi^{(3)}_{11}/\chi^{(3)}_{14}$ and $\chi^{(3)}_{22}/\chi^{(3)}_{14}$ were extracted from the measurements [17,22]:

$$\mathcal{M}^{(3)}_{\text{hex}} = \left(\chi^{(3)}_{14}\right)^2 \begin{pmatrix} \frac{\sqrt{2}}{4}(a^2+b^2+2) & \frac{\sqrt{6}}{12}(a^2+b^2-2) & \frac{\sqrt{3}}{6}(a^2+b^2-2) & \frac{1}{2}(a^2-b^2) & 0 & b & 0 & 0 & 0 & a & 0 & 0 & 0 & 0 & 0 & 0 \\ \frac{\sqrt{2}}{4}(a^2-b^2) & \frac{\sqrt{6}}{12}(a^2-b^2-4) & \frac{\sqrt{3}}{6}(a^2-b^2+2) & \frac{1}{2}(a^2+b^2) & 0 & -b & 0 & 0 & 0 & a & 0 & 0 & 0 & 0 & 0 & 0 \\ 0 & 0 & 0 & 0 & ab & 0 & 1 & b & a & 0 & 0 & 0 & 0 & 0 & 0 & 0 \\ 0 & 0 & 0 & 0 & 0 & 0 & 0 & 0 & 0 & 0 & ab & 0 & -1 & -b & a & 0 \end{pmatrix}. \tag{19}$$

IV. EXTRACTION OF THIRD-ORDER SUSCEPTIBILITIES AND PHASES FROM THE MUELLER MATRIX

Following the derivations analogous to the two-photon and general Stokes-Mueller polarimetry [7–9,23], the expression for third-order susceptibility tensor elements can be obtained from the triple Mueller matrix elements. In deriving the expression for products of a pair of the susceptibility tensor elements, first matrices $\mathcal{T}$ and Γ are derived by vectorizing the Pauli τ and γ matrices, respectively [see Eqs. (A5) and (A6) in Appendix A]. Both $\mathcal{T}$ and Γ matrices are invertible and obey $\mathcal{T}^{-1} = \frac{1}{2}\mathcal{T}^{\dagger}$ and $\Gamma^{-1} = \frac{1}{2}\Gamma^{\dagger}$, respectively. Next the pairwise products of the susceptibilities can be obtained as

$$\mathrm{X}^{(3)} = \mathcal{T}^{-1}\mathcal{M}^{(3)}\Gamma \tag{20}$$

where the matrix $\mathrm{X}^{(3)}$ is for the ensemble average, as was shown in Eq. (15).

In the elemental form, the susceptibility products can be found using $\mathrm{X}_{ij} = \frac{1}{2}\mathcal{T}^{\dagger}_{it}M_{tN}\Gamma_{Nj}$, where $i = (a-1)2 + b$ and $j = (A-1)4 + B$. Since, $\chi_{aA}\chi^{*}_{bB} = |\chi_{aA}||\chi_{bB}|e^{i(\delta_{aA}-\delta_{bB})}$, then the relative phase between any two susceptibility elements $(\delta_{aA} - \delta_{bB})$ in the case of a nondepolarizing sample can be found according to

$$\begin{aligned}\delta_{aA} - \delta_{aA} = \Delta_{aA,bB} &= \tan^{-1}\left(-\mathrm{i}\frac{\chi_{aA}\chi^{*}_{bB} - \chi_{bB}\chi^{*}_{aA}}{\chi_{aA}\chi^{*}_{bB} + \chi_{bB}\chi^{*}_{aA}}\right)\\ &= \tan^{-1}\left(\mathrm{i}\frac{\mathrm{X}_{kl} - \mathrm{X}_{ij}}{\mathrm{X}_{kl} + \mathrm{X}_{ij}}\right)\\ &= \tan^{-1}\left(\mathrm{i}\frac{\mathcal{T}^{\dagger}_{kt}M_{tN}\Gamma_{Nl} - \mathcal{T}^{\dagger}_{it}M_{tN}\Gamma_{Nj}}{\mathcal{T}^{\dagger}_{kt}M_{tN}\Gamma_{Nl} + \mathcal{T}^{\dagger}_{it}M_{tN}\Gamma_{Nj}}\right)\end{aligned} \tag{21}$$

where $k = (b-1)2 + a$ and $l = (B-1)4 + A$, and summation is performed over repeated indices (note that $\mathrm{i} = \sqrt{-1}$ denotes the imaginary number, while i denotes an index). Equations (20) and (21) show that the products of the susceptibility tensor components and the relative phases between the components can be obtained from the Mueller matrix. In the next section, the description of polarimetric measurements will be presented to obtain the Mueller matrix and $\chi^{(3)}$ tensor values.

V. MEASUREMENT OF TRIPLE MUELLER MATRIX OF THE MEDIUM BY THG POLARIMETRY

In order to find each element of $\mathcal{M}^{(3)}$ matrix, the outgoing Stokes vector is measured for each of the 16 unique incoming polarization states. For each measurement Q, all four components of the outgoing Stokes vector s' have to be recorded. The solution to the third-order Mueller matrix from the polarimetry data is

$$\mathcal{M}^{(3)} = s'S^{-1} \tag{22}$$

where s' is a measured 4×16 matrix containing outgoing Stokes states with components s'_0, s'_1, s'_2, s'_3 in columns for the 16 selected incoming polarization states. S^{-1} is a 16×16 matrix obtained by inverting the matrix for 16 different incoming polarization states. It is necessary to choose unique incoming polarization states that produce an invertible matrix. A set of prepared polarization states composed of 16 different orientations for an incoming radiation that generates an invertible matrix S is shown in Fig. 2. In terms of Poincaré coordinates, the states are as follows: $(\Psi,\Omega) = ([0,0],[\frac{\pi}{2},0],[\frac{\pi}{4},0],[-\frac{\pi}{4},0],[0,\frac{\pi}{4}],[0,-\frac{\pi}{4}],[-\frac{\pi}{8},0],[\frac{\pi}{2},\frac{\pi}{8}],[\frac{\pi}{4},-\frac{\pi}{8}],[\frac{\pi}{8},0],[\frac{3\pi}{8},0],[\frac{\pi}{8},\frac{\pi}{8}],[\frac{\pi}{2},-\frac{\pi}{8}],[\frac{\pi}{4},\frac{\pi}{8}],[0,\frac{\pi}{8}],$ and $[-\frac{\pi}{8},\frac{\pi}{8}])$. Additionally the S matrix expression is given in Eq. (B6) of Appendix B.

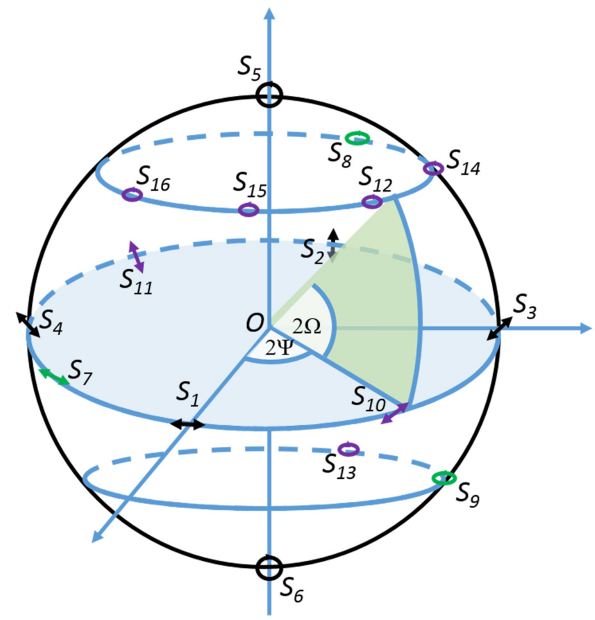

FIG. 2. Poincaré sphere for the triple Stokes vector. States $S_1 \ldots S_{16}$ have the respective Poincaré sphere coordinate values: $(\Psi,\Omega) = ([0,0],[\frac{\pi}{2},0],[\frac{\pi}{4},0],[-\frac{\pi}{4},0],[0,\frac{\pi}{4}],[0,-\frac{\pi}{4}],$ $[-\frac{\pi}{8},0],[\frac{\pi}{2}\frac{\pi}{8}],[\frac{\pi}{4},-\frac{\pi}{8}],[\frac{\pi}{8},0],[\frac{3\pi}{8},0],[\frac{\pi}{8},\frac{\pi}{8}],[\frac{\pi}{2},-\frac{\pi}{8}],$ $[\frac{\pi}{4},\frac{\pi}{8}],[0,\frac{\pi}{8}],$ and $[-\frac{\pi}{8},\frac{\pi}{8}])$. Note S_1 to S_6 states are used for linear polarimetry, and S_1 to S_9 states are also used for the double Stokes vector [9].

A requirement for the Stokes-Mueller polarimetry is finding an invertible matrix using physically realizable incoming polarization states. The proposed set is not unique; however, it does include the six conventional polarization states used for linear polarimetry and the additional three states from SHG polarimetry; in addition seven new states are introduced to form an invertible matrix. Finding an invertible matrix from a set of vectors that represent physical polarization states is not an easy task, and to our knowledge there has not been any analytical solution to this mathematical problem. We have found another set of triple Stokes states, which does not include the previously used states for the linear and double Stokes-Mueller polarimetry, and it is included in Appendix B as an alternative suggestion. Note that the inversion process for extracting the Mueller matrix is susceptible to noise, and therefore the nonlinear polarimetry measurements may require high quality data. Other numerical and analytical approaches to extract the Mueller matrix have been suggested for linear polarimetry and may prove useful for the nonlinear case [24,25]. Numerical optimization methods such as most-likely estimation of the nonlinear susceptibility product matrix from a set of measured outgoing Stokes states can also be employed, similar to the case of multilevel quantum states in the field of quantum tomography [26,27].

The Mueller matrix obtained from the measurements can be used to extract the $\chi^{(3)}$ values and retardance phases using Eqs. (20) and (21), respectively. The extracted $\chi^{(3)}$ values are in the laboratory coordinate frame, and they can be used further to extract the molecular susceptibilities of the structure.

Reduced THG polarimetry with linearly polarized states

For structures with real susceptibilities, the susceptibility component values can be obtained by using only the linear incoming and outgoing polarization states. If the linear incoming polarization state is used, i.e., $s_3 = 0$, then the last six components of the $S^{(3)}$ vector are zero [Eq. (9)]. Therefore, the outgoing s_3' will also be zero for the structure with real-valued susceptibilities [see Eqs. (1), (9), and (17)]. Thus, the reduced Stokes-Mueller polarimetry can be employed for measuring real-valued susceptibility components by conducting the so-called polarization-in polarization-out (PIPO) measurements, where linear polarizations of incoming and outgoing radiation are used. PIPO has been shown to provide a robust determination of the laboratory coordinate susceptibility ratios, the molecular susceptibility ratios, and the orientation angle for cylindrically symmetric materials [17,28,29]. The PIPO setup uses a linear polarizer (at angle θ) for the fundamental radiation, a nonlinear interaction medium, and a linear polarizer (analyzer at an angle φ) for the THG. The THG intensity is measured at different polarizer and analyzer orientations, and the surface plot of intensities is constructed as a function of polarizer and analyzer angles.

The dependence of the outgoing THG Stokes vector on the incoming linear polarization orientation can be derived by multiplying the Mueller matrix from Eq. (17) with the triple Stokes vector of linear polarization [see Appendix B, Eq. (B1)]:

$$\begin{pmatrix} s'_0(3\omega) \\ s'_1(3\omega) \\ s'_2(3\omega) \\ s'_3(3\omega) \end{pmatrix} \propto \begin{pmatrix} \sigma_1^2 + \sigma_2^2 \\ \sigma_1^2 - \sigma_2^2 \\ 2\sigma_1\sigma_2 \\ 0 \end{pmatrix} \tag{23}$$

where

$$\begin{aligned} \sigma_1 &= \chi_{12}^{(3)} \cos(\theta)^3 + 3\,\chi_{14}^{(3)} \cos(\theta)^2 \sin(\theta) \\ &\quad + 3\,\chi_{13}^{(3)} \cos(\theta)\sin(\theta)^2 + \chi_{11}^{(3)} \sin(\theta)^3, \\ \sigma_2 &= \chi_{22}^{(3)} \cos(\theta)^3 + 3\,\chi_{24}^{(3)} \cos(\theta)^2 \sin(\theta) \\ &\quad + 3\,\chi_{23}^{(3)} \cos(\theta)\sin(\theta)^2 + \chi_{21}^{(3)} \sin(\theta)^3. \end{aligned} \tag{24}$$

The resulting THG from the nonlinear medium passing through a linear analyzer is

$$\begin{aligned} s'(3\omega) &= M_{\text{analyzer}}\mathcal{M}^{(3)}S^{(3)}(\theta) \\ &= \mathcal{L}\begin{pmatrix} (\sigma_1 \sin\varphi + \sigma_2 \cos\varphi)^2 \\ \cos(2\varphi)(\sigma_1 \sin\varphi + \sigma_2 \cos\varphi)^2 \\ \sin(2\varphi)(\sigma_1 \sin\varphi + \sigma_2 \cos\varphi)^2 \\ 0 \end{pmatrix} \end{aligned} \tag{25}$$

where $\mathcal{L}$ is a scaling constant accounting for the experimental conditions and is proportional to the intensity of fundamental radiation. From Eq. (25) it follows that for real susceptibilities and linear incoming polarization $s_3' = 0$. Therefore, it is very informative to measure the s_3' component, and if the measured value is negligible real susceptibilities may be assumed for the material. Additionally, $s_3' = 0$ shows that the fundamental and THG radiations do not experience birefringence. Such assumption applies often when measuring thin samples at the wavelength away from the fundamental and THG absorption bands. The s_0' component, expressed in Eq. (25), is similar to the PIPO equation for THG, which has been used previously to investigate crystalline structures [17,22]. It can be used in nonlinear microscopy to fit the PIPO surface plot of THG imaging data, and is more explicitly stated as follows:

$$s_0'(3\omega) = I_{3\omega}(\theta,\varphi) = \mathcal{L}|\sigma_1 \sin\varphi + \sigma_2 \cos\varphi|^2. \tag{26}$$

For a sample with isotropic symmetry, there is only one independent susceptibility ($\chi_{11}^{(3)} = \chi_{22}^{(3)} = 3\chi_{14}^{(3)}$):

$$\begin{aligned} s_0'(3\omega)_{\text{iso}} &\propto \left|\chi_{11}^{(3)}\right|^2 |\cos(\varphi)\cos(\theta) + \sin(\varphi)\sin(\theta)|^2 \\ &\propto |\cos(\varphi - \theta)|^2. \end{aligned} \tag{27}$$

Thus, for isotropically symmetric material the outgoing intensity directly depends only on the direction of incoming radiation and scales according to an effective susceptibility. This predication can be tested in an experiment. The isotropic distribution of retinal molecules in the fruit fly eye and the astaxanthin molecules in red aplanospores of *Haematococcus pluvialis* has been observed with THG polarimetric microscopy [17,22].

For hexagonally symmetric samples, where Kleinman symmetry is also valid, there are three independent nonzero susceptibilities ($\chi_{11}^{(3)}, \chi_{22}^{(3)}$, and $\chi_{14}^{(3)}$):

$$\begin{aligned} s_0'(3\omega)_{\text{hex}} \propto\ & \big|\cos(\varphi)\big(\chi_{22}^{(3)}\cos(\theta)^3 + 3\chi_{14}^{(3)}\cos(\theta)\sin(\theta)^2\big) \\ & + \sin(\varphi)\big(3\chi_{14}^{(3)}\cos(\theta)^2\sin(\theta) + \chi_{11}^{(3)}\sin(\theta)^3\big)\big|^2. \end{aligned} \tag{28}$$

This relation can be used to fit the two-dimensional (θ,φ) intensity (PIPO) surface plot when performing polarimetry for a sample possessing hexagonal symmetry such as H aggregates of astaxanthin and β-carotene aggregates in orange carrot root cells [17,22].

VI. DISCUSSION AND CONCLUSION

The three-photon polarimetry equations, just like in two-photon polarimetry, follow from the general Stokes-Mueller polarimetry formalism [8]. The dimensions of the coherency matrix, the polarization state vector, and the material matrix are larger for the three-photon compared to the two-photon polarimetry. The 4×4 γ matrices expand the coherency matrix as well as the corresponding Mueller matrix. The Mueller matrix $\mathcal{M}^{(3)}$ and polarization state vector $S^{(3)}$ have 4×16 and 16×1 dimensions, respectively. Similar to two-photon polarimetry, the $\mathcal{M}^{(3)}$- and $\mathrm{X}^{(3)}$-matrix components can be sorted into four groups (NP, I, O, and OI) with distinct phase relations between the incoming and outgoing retardance effects.

A complete three-photon polarimetry experiment utilizes a set of 16 unique polarization states of incoming radiation each composed of 16 triple Stokes vector elements, which forms an invertible matrix, with numerical values given in Eq. (B6) in Appendix B. This 16×16 matrix is used together with the outgoing polarization states s' to determine uniquely all elements of the material matrix $\mathcal{M}^{(3)}$. For the material with real susceptibilities, and when Kleinman symmetry is valid, the Mueller matrix is composed of five independent susceptibility tensor elements, and it reduces to four ratios. Therefore, all 64 elements of matrix $\mathcal{M}^{(3)}$ are not independent. In addition, by a reduced polarimetry a subset of $\mathcal{M}^{(3)}$ components may be exploited to determine the susceptibility ratios for certain material symmetries. For instance, PIPO measurements, with linearly polarized states of incoming and outgoing radiations, can be used to deduce the real-valued susceptibilities in cylindrically symmetric materials [17,22].

For the isotropically symmetric materials, the Mueller matrix is composed of constants, independent of susceptibilities, and the THG signal scales with an effective susceptibility [Eq. (18)]. Thus, the outgoing radiation has a simple dependence on the $\mathcal{M}^{(3)}$ matrix, and the matrix component values can be easily verified experimentally with the polarimetric measurement in isotropic media. The triple Mueller matrix of hexagonally symmetric material depends on two ratios, and some elements depend only on a single ratio. Therefore, in designing experiments for a material possessing hexagonal symmetry, a reduced polarimetry may be conducted to obtain the susceptibility component ratios, using only a few polarization states of incoming and outgoing radiation.

In summary, we presented a framework for the triple Stokes-Mueller polarimetry of three-photon processes. The theory is provided in the context and in analogy with previous works on Stokes-Mueller formalism as well as conventional nonlinear optics notations [8,9]. The derived equations relate the outgoing Stokes vector for the THG signal to the polarization state of the incoming fundamental radiation beam and to the third-order susceptibility tensor values of the intervening medium. We have additionally described the method for performing a complete three-photon Stokes-Mueller polarimetry, which requires 16 independent polarization states for the incoming radiation. Various symmetries of a material can be explored with expressions of a triple Mueller matrix, and consequently a reduced polarimetry may be performed for known symmetries to extract the corresponding susceptibility ratios and orientations of the principle axis of the material.

The triple Stokes-Mueller polarimetry can be extended to other three-photon processes as well, including CARS, by redefining the polarization state vector for incoming radiation. However, the validity of the intensity independent susceptibilities has to be tested by performing experiments with different incoming radiation intensities, especially when the incoming radiation wavelength approaches resonant transitions of the molecules in the material. The extension of three-photon polarimetry to other nonlinear processes provides a great opportunity for future research into triple Stokes-Mueller polarimetry.

ACKNOWLEDGMENTS

The authors would like to thank Prof. Daniel James from the University of Toronto for useful discussions. This work was supported by grants from the Natural Sciences and Engineering Research Council of Canada (NSERC) and the Canadian Institutes of Health Research (CIHR). M.S. acknowledges financial support from the Ontario Graduate Scholarship (OGS).

APPENDIX A: PAULI AND GAMMA MATRICES

Three-photon polarimetry requires the expansion of the coherency matrix for the incoming and outgoing radiation to obtain the corresponding real-valued Stokes vector components, as well as the triple Mueller matrix elements. Due to a size difference between the dimension of the matrices for the incoming and outgoing radiations, the corresponding expansions are also different. The outgoing radiation is expanded by the conventional 2×2 τ matrices, also known as Pauli matrices, while the incoming radiation and $\mathcal{M}^{(3)}$ require 4×4 γ matrices.

Following the recipe as described in Ref. [8], the γ matrices for three-photon polarimetry are developed in two steps: First, the matrix γ''_{jk} is defined such that only the value of element jk of the matrix γ''_{jk} is one, and it is zero for all other elements (both j and k run from 1 to 4). These two-dimensional sets of matrices are shown in Eq. (A1), where each element of the set is a 4×4 matrix.

$$\begin{aligned}
\gamma''_{1,1} &= \begin{pmatrix} 1&0&0&0\\0&0&0&0\\0&0&0&0\\0&0&0&0 \end{pmatrix} & \gamma''_{1,2} &= \begin{pmatrix} 0&1&0&0\\0&0&0&0\\0&0&0&0\\0&0&0&0 \end{pmatrix} & \gamma''_{1,3} &= \begin{pmatrix} 0&0&1&0\\0&0&0&0\\0&0&0&0\\0&0&0&0 \end{pmatrix} & \gamma''_{1,4} &= \begin{pmatrix} 0&0&0&1\\0&0&0&0\\0&0&0&0\\0&0&0&0 \end{pmatrix}\\
\gamma''_{2,1} &= \begin{pmatrix} 0&0&0&0\\1&0&0&0\\0&0&0&0\\0&0&0&0 \end{pmatrix} & \gamma''_{2,2} &= \begin{pmatrix} 0&0&0&0\\0&1&0&0\\0&0&0&0\\0&0&0&0 \end{pmatrix} & \gamma''_{2,3} &= \begin{pmatrix} 0&0&0&0\\0&0&1&0\\0&0&0&0\\0&0&0&0 \end{pmatrix} & \gamma''_{2,4} &= \begin{pmatrix} 0&0&0&0\\0&0&0&1\\0&0&0&0\\0&0&0&0 \end{pmatrix}\\
\gamma''_{3,1} &= \begin{pmatrix} 0&0&0&0\\0&0&0&0\\1&0&0&0\\0&0&0&0 \end{pmatrix} & \gamma''_{3,2} &= \begin{pmatrix} 0&0&0&0\\0&0&0&0\\0&1&0&0\\0&0&0&0 \end{pmatrix} & \gamma''_{3,3} &= \begin{pmatrix} 0&0&0&0\\0&0&0&0\\0&0&1&0\\0&0&0&0 \end{pmatrix} & \gamma''_{3,4} &= \begin{pmatrix} 0&0&0&0\\0&0&0&0\\0&0&0&1\\0&0&0&0 \end{pmatrix}\\
\gamma''_{4,1} &= \begin{pmatrix} 0&0&0&0\\0&0&0&0\\0&0&0&0\\1&0&0&0 \end{pmatrix} & \gamma''_{4,2} &= \begin{pmatrix} 0&0&0&0\\0&0&0&0\\0&0&0&0\\0&1&0&0 \end{pmatrix} & \gamma''_{4,3} &= \begin{pmatrix} 0&0&0&0\\0&0&0&0\\0&0&0&0\\0&0&1&0 \end{pmatrix} & \gamma''_{4,4} &= \begin{pmatrix} 0&0&0&0\\0&0&0&0\\0&0&0&0\\0&0&0&1 \end{pmatrix}
\end{aligned}. \tag{A1}$$

Note that γ'' matrices can also expand the coherency matrix $\rho^{(3)}$ of Eq. (7). However, the resulting vector for $S^{(3)}$ and $\mathcal{M}^{(3)}$ matrices will be complex. Thus, in a second step, the desired Hermitian matrices for a third-order process are obtained using the following relations for the two-dimensional γ' matrices:

$$\gamma'_{jk} = \begin{cases} \gamma''_{jk} + \gamma''_{kj}, & \text{if } j < k \\ \mathrm{i}(\gamma''_{jk} - \gamma''_{kj}), & \text{if } j > k \\ \sqrt{\frac{2}{j^2+j}}\left[\left(\sum_{m=1}^{j} \gamma''_{mm}\right) - j\gamma''_{j+1,j+1}\right], & \text{if } 1 \leqslant k = j < 4 \\ \frac{1}{\sqrt{2}}\mathcal{I}_4, & \text{if } j = k = 4 \end{cases} \tag{A2}$$

where $\mathcal{I}_4$ is the 4×4 identity matrix. When $j < k$, $\gamma'_{jk} = \gamma''_{jk} + \gamma''_{kj}$ matrices are real; when $j > k$, $\gamma'_{jk} = \mathrm{i}(\gamma''_{jk} - \gamma''_{kj})$ matrices are complex, and have similar nonzero elements as in their real-value counterparts; when $1 \leqslant j = k < 4$), the obtained γ'_{jk} matrices are diagonal and real, including when $j = k = 4$ that generates the identity matrix.

The two-dimensional γ' set is then converted to a one-dimensional set of matrices [30]: $\gamma'_{jk} \to \gamma_N$, where $N = 1,\ldots,16$. In Eq. (A3), the two-dimensional 4×4 γ' set is shown but labeled with the one-dimensional 16-element set γ. The presented order of γ matrices in Eq. (A3) is chosen to remain consistent with the order of the linear Stokes vector [determined by Pauli matrices in Eq. (A4)] as well as the second-order Stokes vector (determined by Gell-Mann matrices in Ref. [9]). These matrices satisfy all the requirements as desired for expanding the coherency matrix for the nonlinear polarimetry. In addition, they ensure that γ obeys $\mathrm{Tr}(\gamma_M\gamma_N) = 2\delta_{MN}$:

$$\begin{array}{llll}
\gamma_4 = \begin{pmatrix} 1 & 0 & 0 & 0 \\ 0 & -1 & 0 & 0 \\ 0 & 0 & 0 & 0 \\ 0 & 0 & 0 & 0 \end{pmatrix} &
\gamma_5 = \begin{pmatrix} 0 & 1 & 0 & 0 \\ 1 & 0 & 0 & 0 \\ 0 & 0 & 0 & 0 \\ 0 & 0 & 0 & 0 \end{pmatrix} &
\gamma_9 = \begin{pmatrix} 0 & 0 & 1 & 0 \\ 0 & 0 & 0 & 0 \\ 1 & 0 & 0 & 0 \\ 0 & 0 & 0 & 0 \end{pmatrix} &
\gamma_{10} = \begin{pmatrix} 0 & 0 & 0 & 1 \\ 0 & 0 & 0 & 0 \\ 0 & 0 & 0 & 0 \\ 1 & 0 & 0 & 0 \end{pmatrix} \\
\gamma_{11} = \begin{pmatrix} 0 & -\mathrm{i} & 0 & 0 \\ \mathrm{i} & 0 & 0 & 0 \\ 0 & 0 & 0 & 0 \\ 0 & 0 & 0 & 0 \end{pmatrix} &
\gamma_3 = \frac{\sqrt{3}}{3}\begin{pmatrix} 1 & 0 & 0 & 0 \\ 0 & 1 & 0 & 0 \\ 0 & 0 & -2 & 0 \\ 0 & 0 & 0 & 0 \end{pmatrix} &
\gamma_6 = \begin{pmatrix} 0 & 0 & 0 & 0 \\ 0 & 0 & 1 & 0 \\ 0 & 1 & 0 & 0 \\ 0 & 0 & 0 & 0 \end{pmatrix} &
\gamma_8 = \begin{pmatrix} 0 & 0 & 0 & 0 \\ 0 & 0 & 0 & 1 \\ 0 & 0 & 0 & 0 \\ 0 & 1 & 0 & 0 \end{pmatrix} \\
\gamma_{15} = \begin{pmatrix} 0 & 0 & -\mathrm{i} & 0 \\ 0 & 0 & 0 & 0 \\ \mathrm{i} & 0 & 0 & 0 \\ 0 & 0 & 0 & 0 \end{pmatrix} &
\gamma_{12} = \begin{pmatrix} 0 & 0 & 0 & 0 \\ 0 & 0 & -\mathrm{i} & 0 \\ 0 & \mathrm{i} & 0 & 0 \\ 0 & 0 & 0 & 0 \end{pmatrix} &
\gamma_2 = \frac{\sqrt{6}}{6}\begin{pmatrix} 1 & 0 & 0 & 0 \\ 0 & 1 & 0 & 0 \\ 0 & 0 & 1 & 0 \\ 0 & 0 & 0 & -3 \end{pmatrix} &
\gamma_7 = \begin{pmatrix} 0 & 0 & 0 & 0 \\ 0 & 0 & 0 & 0 \\ 0 & 0 & 0 & 1 \\ 0 & 0 & 1 & 0 \end{pmatrix}. \\
\gamma_{16} = \begin{pmatrix} 0 & 0 & 0 & -\mathrm{i} \\ 0 & 0 & 0 & 0 \\ 0 & 0 & 0 & 0 \\ \mathrm{i} & 0 & 0 & 0 \end{pmatrix} &
\gamma_{14} = \begin{pmatrix} 0 & 0 & 0 & 0 \\ 0 & 0 & 0 & -\mathrm{i} \\ 0 & 0 & 0 & 0 \\ 0 & \mathrm{i} & 0 & 0 \end{pmatrix} &
\gamma_{13} = \begin{pmatrix} 0 & 0 & 0 & 0 \\ 0 & 0 & 0 & 0 \\ 0 & 0 & 0 & -\mathrm{i} \\ 0 & 0 & \mathrm{i} & 0 \end{pmatrix} &
\gamma_1 = \frac{\sqrt{2}}{2}\begin{pmatrix} 1 & 0 & 0 & 0 \\ 0 & 1 & 0 & 0 \\ 0 & 0 & 1 & 0 \\ 0 & 0 & 0 & 1 \end{pmatrix}
\end{array} \tag{A3}$$

The Pauli τ matrices and 2×2 identity matrix are special cases of η matrices with dimension 2 [8]. They have the orthogonal property $\mathrm{Tr}(\tau_\mu\tau_\nu) = 2\delta_{\mu\nu}$, where $\delta_{\mu\nu}$ is the Kronecker delta:

$$\begin{array}{ll} \tau_0 = \begin{pmatrix} 1 & 0 \\ 0 & 1 \end{pmatrix} & \tau_1 = \begin{pmatrix} 1 & 0 \\ 0 & -1 \end{pmatrix} \\ \tau_2 = \begin{pmatrix} 0 & 1 \\ 1 & 0 \end{pmatrix} & \tau_3 = \begin{pmatrix} 0 & -\mathrm{i} \\ \mathrm{i} & 0 \end{pmatrix} \end{array}. \tag{A4}$$

The matrix $\mathcal{T}$, used in Sec. IV to derive the susceptibility tensor elements in terms of the Mueller matrix, is obtained by the vectorization operation, where each row of the matrix $\mathcal{T}$ comes from the Pauli matrices. $\mathcal{T}$ is invertible and obeys $\mathcal{T}^{-1} = \frac{1}{2}\mathcal{T}^{\dagger}$:

$$\mathcal{T} \equiv (\mathrm{vec}(\tau_0), \cdots, \mathrm{vec}(\tau_3))^T = \begin{pmatrix} 1 & 0 & 0 & 1 \\ 1 & 0 & 0 & -1 \\ 0 & 1 & 1 & 0 \\ 0 & \mathrm{i} & -\mathrm{i} & 0 \end{pmatrix}. \tag{A5}$$

In Sec. IV matrices $\mathcal{T}$ and Γ are used to derive the third-order susceptibilities and their phases in terms of the triple Mueller matrix elements. Γ is derived from γ matrices [Eq. (A3)], where each row of Γ is expressed by vectorizing γ matrices. Γ is invertible and $\Gamma^{-1} = \frac{1}{2}\Gamma^{\dagger}$:

$$\Gamma \equiv (\text{vec}(\gamma_1), \text{vec}(\gamma_2), \ldots, \text{vec}(\gamma_{15}), \text{vec}(\gamma_{16}))^T$$
$$= \begin{pmatrix}
\frac{\sqrt{2}}{2} & 0 & 0 & 0 & 0 & \frac{\sqrt{2}}{2} & 0 & 0 & 0 & 0 & \frac{\sqrt{2}}{2} & 0 & 0 & 0 & 0 & \frac{\sqrt{2}}{2} \\
\frac{\sqrt{6}}{6} & 0 & 0 & 0 & 0 & \frac{\sqrt{6}}{6} & 0 & 0 & 0 & 0 & \frac{\sqrt{6}}{6} & 0 & 0 & 0 & 0 & \frac{-3}{\sqrt{6}} \\
\frac{\sqrt{3}}{3} & 0 & 0 & 0 & 0 & \frac{\sqrt{3}}{3} & 0 & 0 & 0 & 0 & \frac{-2}{\sqrt{3}} & 0 & 0 & 0 & 0 & 0 \\
1 & 0 & 0 & 0 & 0 & -1 & 0 & 0 & 0 & 0 & 0 & 0 & 0 & 0 & 0 & 0 \\
0 & 1 & 0 & 0 & 1 & 0 & 0 & 0 & 0 & 0 & 0 & 0 & 0 & 0 & 0 & 0 \\
0 & 0 & 0 & 0 & 0 & 0 & 1 & 0 & 0 & 1 & 0 & 0 & 0 & 0 & 0 & 0 \\
0 & 0 & 0 & 0 & 0 & 0 & 0 & 0 & 0 & 0 & 0 & 1 & 0 & 0 & 1 & 0 \\
0 & 0 & 0 & 0 & 0 & 0 & 0 & 1 & 0 & 0 & 0 & 0 & 0 & 1 & 0 & 0 \\
0 & 0 & 1 & 0 & 0 & 0 & 0 & 0 & 1 & 0 & 0 & 0 & 0 & 0 & 0 & 0 \\
0 & 0 & 0 & 1 & 0 & 0 & 0 & 0 & 0 & 0 & 0 & 0 & 1 & 0 & 0 & 0 \\
0 & \mathrm{i} & 0 & 0 & -\mathrm{i} & 0 & 0 & 0 & 0 & 0 & 0 & 0 & 0 & 0 & 0 & 0 \\
0 & 0 & 0 & 0 & 0 & 0 & \mathrm{i} & 0 & 0 & -\mathrm{i} & 0 & 0 & 0 & 0 & 0 & 0 \\
0 & 0 & 0 & 0 & 0 & 0 & 0 & 0 & 0 & 0 & 0 & \mathrm{i} & 0 & 0 & -\mathrm{i} & 0 \\
0 & 0 & 0 & 0 & 0 & 0 & 0 & \mathrm{i} & 0 & 0 & 0 & 0 & 0 & -\mathrm{i} & 0 & 0 \\
0 & 0 & \mathrm{i} & 0 & 0 & 0 & 0 & 0 & -\mathrm{i} & 0 & 0 & 0 & 0 & 0 & 0 & 0 \\
0 & 0 & 0 & \mathrm{i} & 0 & 0 & 0 & 0 & 0 & 0 & 0 & 0 & -\mathrm{i} & 0 & 0 & 0
\end{pmatrix}. \tag{A6}$$

APPENDIX B: $S^{(3)}$ VECTOR FOR VARIOUS POLARIZATIONS

1. Triple Stokes for linearly polarized states

When the incoming electric field is linearly polarized at an angle θ from the primary axis, $E(\omega) = [E_1(\omega), E_2(\omega)]^T = E_0[\sin\theta, \cos\theta]^T$. Substituting this in Eq. (9), the linearly polarized incoming state for THG is

$$S^{(3)}(\theta) = \langle E_0^6 \rangle \begin{pmatrix}
\frac{\sqrt{2}}{2}[\cos(\theta)^6 + 9\cos(\theta)^4\sin(\theta)^2 + 9\cos(\theta)^2\sin(\theta)^4 + \sin(\theta)^6] \\
\frac{\sqrt{6}}{6}[\cos(\theta)^6 - 27\cos(\theta)^4\sin(\theta)^2 + 9\cos(\theta)^2\sin(\theta)^4 + \sin(\theta)^6] \\
\frac{\sqrt{3}}{3}[\cos(\theta)^6 - 18\cos(\theta)^2\sin(\theta)^4 + \sin(\theta)^6] \\
\sin(\theta)^6 - \cos(\theta)^6 \\
2\cos(\theta)^3\sin(\theta)^3 \\
6\cos(\theta)^4\sin(\theta)^2 \\
18\cos(\theta)^3\sin(\theta)^3 \\
6\cos(\theta)^5\sin(\theta) \\
6\cos(\theta)\sin(\theta)^5 \\
6\cos(\theta)^2\sin(\theta)^4 \\
0 \\
0 \\
0 \\
0 \\
0 \\
0
\end{pmatrix}. \tag{B1}$$

Multiplying Eqs. (B1) and (17), the outgoing THG Stokes vector is obtained as shown in Eq. (23). The outgoing Stokes vector shows that by using incoming linearly polarized states the outgoing polarization will also be linear, i.e., $s'_3 = 0$ in Eq. (23). This feature is used in linear PIPO measurements as described in Sec. V.

2. Triple Stokes vector on Poincaré sphere

The Poincaré sphere is a useful geometrical representation by which different polarization states can be visually identified. In addition, in order to determine values of the Mueller matrix $\mathcal{M}^{(3)}$ elements from polarimetry measurements, numerical values for the incoming polarization states are required [see Eq. (22)]. The numerical values can be obtained by deriving the triple Stokes vector in terms of Poincaré coordinates in general, and subsequently evaluating triple Stokes vector elements values by substituting the corresponding state's coordinates. The Stokes vector in the Poincaré sphere coordinates is

$$s = \langle E_0^2 \rangle \begin{pmatrix} 1 \\ \cos(2\Psi)\cos(2\Omega) \\ \sin(2\Psi)\cos(2\Omega) \\ \sin(2\Omega) \end{pmatrix} \tag{B2}$$

where the variables 2Ψ and 2Ω are the azimuth and latitude coordinates on the Poincaré sphere as shown in Fig. 2. The triple Stokes vector in terms of Poincaré coordinates is derived by substituting s values from Eq. (B2) into Eq. (9) and is shown in Eq. (B3).

3. The Matrix of prepared triple Stokes elements for complete Mueller polarimetry measurement

The matrix composed of triple Stokes states to perform a complete polarimetry measurement has to be invertible. One invertible matrix can be constructed from the 16 polarization states given by the Poincaré coordinates in Eq. (B4) and shown on the Poincaré sphere in Fig. 2. By substituting these coordinates into Eq. (B2), the 4×1 Stokes vector values are obtained as in Eq. (B5). Furthermore, by substituting the Poincaré coordinate values from Eq. (B4) into Eq. (B3) below, the triple Stokes vector values for the 16 states are obtained [see Eq. (B6)]:

$$S^{(3)}(\Psi,\Omega) = \tfrac{1}{4}\langle {E_0}^6 \rangle = \begin{pmatrix} \sqrt{2}[5 - 3\cos(2\,\Omega)^2\cos(2\,\Psi)^2] \\ \sqrt{6}\left[-3\cos(2\,\Omega)^3\cos(2\,\Psi)^3 + 2\cos(2\,\Omega)^2\cos(2\,\Psi)^2 + 3\cos(2\,\Omega)\,\cos(2\,\Psi) - \frac{4}{3}\right] \\ \sqrt{3}\left[3\cos(2\,\Omega)^3\cos(2\,\Psi)^3 + 4\cos(2\,\Omega)^2\cos(2\,\Psi)^2 - 3\cos(2\,\Omega)\,\cos(2\,\Psi) - \frac{8}{3}\right] \\ \cos(2\,\Omega)^3\cos(2\,\Psi)^3 + 3\,\cos(2\,\Omega)\,\cos(2\,\Psi) \\ \cos(2\,\Omega)^3\sin(2\,\Psi)^3 - 3\,\cos(2\,\Omega)\sin(2\,\Omega)^2\,\sin(2\,\Psi) \\ 3\,(\cos(2\,\Omega)\,\cos(2\,\Psi) - 1)\,(\cos(2\,\Omega)^2\,(\cos(2\,\Psi)^2 - 1) - \cos(2\,\Omega)^2 + 1) \\ -9\,\cos(2\,\Omega)\,\sin(2\,\Psi)\,(\cos(2\,\Omega)^2\cos(2\,\Psi)^2 - 1) \\ 3\,\cos(2\,\Omega)\,\sin(2\,\Psi)\,(\cos(2\,\Omega)\,\cos(2\,\Psi) - 1)^2 \\ 3\,\cos(2\,\Omega)\,\sin(2\,\Psi)\,(\cos(2\,\Omega)\,\cos(2\,\Psi) + 1)^2 \\ -3\,(\cos(2\,\Omega)\,\cos(2\,\Psi) + 1)\,(\cos(2\,\Omega)^2\,(\cos(2\,\Psi)^2 - 1) - \cos(2\,\Omega)^2 + 1) \\ -\sin(2\,\Omega)^3 + 3\,\sin(2\,\Omega)\sin(2\,\Psi)^2\,(\sin(2\,\Omega)^2 - 1) \\ 6\,\cos(2\,\Omega)\,\sin(2\,\Omega)\,\sin(2\,\Psi)\,(\cos(2\,\Omega)\,\cos(2\,\Psi) - 1) \\ -9\,\sin(2\,\Omega)\,((\sin(2\,\Omega)^2 - 1)\,(\sin(2\,\Psi)^2 - 1) - 1) \\ -3\,\sin(2\,\Omega)\,(\cos(2\,\Omega)\,\cos(2\,\Psi) - 1)^2 \\ 3\,\sin(2\,\Omega)\,(\cos(2\,\Omega)\,\cos(2\,\Psi) + 1)^2 \\ 6\,\cos(2\,\Omega)\,\sin(2\,\Omega)\,\sin(2\,\Psi)\,(\cos(2\,\Omega)\,\cos(2\,\Psi) + 1) \end{pmatrix}. \tag{B3}$$

The 16×16 matrix S of the triple Stokes states, given in Eq. (B6), can be used in polarimetric measurements to recover the triple Mueller matrix values according to Eq. (22). The chosen triple Stokes states include the states that also are used for linear and double Stokes polarimetry [9]. However, other states can be used as long as the corresponding 16×16 matrix defined by the triple Stokes polarization states is invertible for use in Eq. (22). An alternative set is $(\Gamma,\Omega)_Q = ([0,0],[\frac{\pi}{2},0],[\frac{\pi}{4},0],[-\frac{\pi}{4},0],[0,\frac{\pi}{4}],[0,-\frac{\pi}{4}],[-\frac{\pi}{8},0],[\frac{3\pi}{8},0],[0,\frac{\pi}{8}],[\frac{\pi}{2},-\frac{\pi}{8}],[\frac{\pi}{4},\frac{\pi}{8}],[-\frac{\pi}{4},-\frac{\pi}{8}],[\frac{3\pi}{8},\frac{\pi}{8}],[\frac{\pi}{2},\frac{\pi}{8}],[\frac{\pi}{8},0],[\frac{\pi}{8},\frac{\pi}{8}])$.

In terms of Poincaré coordinates one set for the triple Stokes vector states is (also shown in Fig. 2)

$$((\Psi,\Omega)_Q) = \Big([0,0],\Big[\frac{\pi}{2},0\Big],\Big[\frac{\pi}{4},0\Big],\Big[-\frac{\pi}{4},0\Big],\Big[0,\frac{\pi}{4}\Big],\Big[0,-\frac{\pi}{4}\Big],\Big[-\frac{\pi}{8},0\Big],\Big[\frac{\pi}{2},\frac{\pi}{8}\Big],\Big[\frac{\pi}{4},-\frac{\pi}{8}\Big],\Big[\frac{\pi}{8},0\Big],\Big[\frac{3\pi}{8},0\Big],\Big[\frac{\pi}{8},\frac{\pi}{8}\Big], \Big[\frac{\pi}{2},-\frac{\pi}{8}\Big],\Big[\frac{\pi}{4},\frac{\pi}{8}\Big],\Big[0,\frac{\pi}{8}\Big],\Big[-\frac{\pi}{8},\frac{\pi}{8}\Big]\Big), \tag{B4}$$

$$(\mathbf{s}_{t,Q}) = (\mathbf{s}_{t,1}\quad \mathbf{s}_{t,2}\quad \mathbf{s}_{t,3}\quad \mathbf{s}_{t,4}\quad \mathbf{s}_{t,5}\quad \mathbf{s}_{t,6}\quad \mathbf{s}_{t,7}\quad \mathbf{s}_{t,8}\quad \mathbf{s}_{t,9}\quad \mathbf{s}_{t,10}\quad \mathbf{s}_{t,11}\quad \mathbf{s}_{t,12}\quad \mathbf{s}_{t,13}\quad \mathbf{s}_{t,14}\quad \mathbf{s}_{t,15}\quad \mathbf{s}_{t,16})$$

$$\begin{pmatrix} s_{0,Q}\\ s_{1,Q}\\ s_{2,Q}\\ s_{3,Q}\end{pmatrix} \propto \langle E_0^2\rangle \begin{pmatrix} 1 & 1 & 1 & 1 & 1 & 1 & 1 & 1 & 1 & 1 & 1 & 1 & 1 & 1 & 1 & 1\\ 1 & -1 & 0 & 0 & 0 & 0 & \frac{\sqrt{2}}{2} & -\frac{\sqrt{2}}{2} & 0 & \frac{\sqrt{2}}{2} & -\frac{\sqrt{2}}{2} & \frac{1}{2} & -\frac{\sqrt{2}}{2} & 0 & \frac{\sqrt{2}}{2} & \frac{1}{2}\\ 0 & 0 & 1 & -1 & 0 & 0 & -\frac{\sqrt{2}}{2} & 0 & \frac{\sqrt{2}}{2} & \frac{\sqrt{2}}{2} & \frac{\sqrt{2}}{2} & \frac{1}{2} & 0 & \frac{\sqrt{2}}{2} & 0 & -\frac{1}{2}\\ 0 & 0 & 0 & 0 & 1 & -1 & 0 & \frac{\sqrt{2}}{2} & -\frac{\sqrt{2}}{2} & 0 & 0 & \frac{\sqrt{2}}{2} & -\frac{\sqrt{2}}{2} & \frac{\sqrt{2}}{2} & \frac{\sqrt{2}}{2} & \frac{\sqrt{2}}{2} \end{pmatrix}, \tag{B5}$$

$$\begin{pmatrix} S_{1,Q}\\ S_{2,Q}\\ S_{3,Q}\\ S_{4,Q}\\ S_{5,Q}\\ S_{6,Q}\\ S_{7,Q}\\ S_{8,Q}\\ S_{9,Q}\\ S_{10,Q}\\ S_{11,Q}\\ S_{12,Q}\\ S_{13,Q}\\ S_{14,Q}\\ S_{15,Q}\\ S_{16,Q}\end{pmatrix} \propto \langle E_0^6\rangle \begin{pmatrix}
\frac{\sqrt{2}}{2} & \frac{\sqrt{2}}{2} & \frac{5\sqrt{2}}{4} & \frac{5\sqrt{2}}{4} & \frac{5\sqrt{2}}{4} & \frac{5\sqrt{2}}{4} & \frac{7\sqrt{2}}{8} & \frac{7\sqrt{2}}{8} & \frac{5\sqrt{2}}{4} & \frac{7\sqrt{2}}{8} & \frac{7\sqrt{2}}{8} & \frac{17\sqrt{2}}{16} & \frac{7\sqrt{2}}{8} & \frac{5\sqrt{2}}{4} & \frac{7\sqrt{2}}{8} & \frac{17\sqrt{2}}{16}\\
\frac{\sqrt{6}}{6} & \frac{\sqrt{6}}{6} & -\frac{\sqrt{6}}{3} & -\frac{\sqrt{6}}{3} & -\frac{\sqrt{6}}{3} & -\frac{\sqrt{6}}{3} & \frac{\sqrt{6}(9\sqrt{2}-4)}{48} & -\frac{\sqrt{6}(9\sqrt{2}+4)}{48} & -\frac{\sqrt{6}}{3} & \frac{\sqrt{6}(9\sqrt{2}-4)}{48} & -\frac{\sqrt{6}(9\sqrt{2}+4)}{48} & \frac{7\sqrt{6}}{96} & -\frac{\sqrt{6}(9\sqrt{2}+4)}{48} & -\frac{\sqrt{6}}{3} & \frac{\sqrt{6}(9\sqrt{2}-4)}{48} & \frac{7\sqrt{6}}{96}\\
\frac{\sqrt{3}}{3} & \frac{\sqrt{3}}{3} & -\frac{2\sqrt{3}}{3} & -\frac{2\sqrt{3}}{3} & -\frac{2\sqrt{3}}{3} & -\frac{2\sqrt{3}}{3} & -\frac{\sqrt{3}(9\sqrt{2}+8)}{48} & \frac{\sqrt{3}(9\sqrt{2}-8)}{48} & -\frac{2\sqrt{3}}{3} & -\frac{\sqrt{3}(9\sqrt{2}+8)}{48} & \frac{\sqrt{3}(9\sqrt{2}-8)}{48} & -\frac{67\sqrt{3}}{96} & \frac{\sqrt{3}(9\sqrt{2}-8)}{48} & -\frac{2\sqrt{3}}{3} & -\frac{\sqrt{3}(9\sqrt{2}+8)}{48} & -\frac{67\sqrt{3}}{96}\\
1 & -1 & 0 & 0 & 0 & 0 & \frac{7\sqrt{2}}{16} & -\frac{7\sqrt{2}}{16} & 0 & \frac{7\sqrt{2}}{16} & -\frac{7\sqrt{2}}{16} & \frac{13}{32} & -\frac{7\sqrt{2}}{16} & 0 & \frac{7\sqrt{2}}{16} & \frac{13}{32}\\
0 & 0 & \frac{1}{4} & -\frac{1}{4} & 0 & 0 & -\frac{\sqrt{2}}{16} & 0 & -\frac{\sqrt{2}}{8} & \frac{\sqrt{2}}{16} & \frac{\sqrt{2}}{16} & -\frac{5}{32} & 0 & -\frac{\sqrt{2}}{8} & 0 & \frac{5}{32}\\
0 & 0 & \frac{3}{4} & \frac{3}{4} & -\frac{3}{4} & -\frac{3}{4} & \frac{3}{8}-\frac{3\sqrt{2}}{16} & -\frac{3\sqrt{2}}{16}-\frac{3}{8} & 0 & \frac{3}{8}-\frac{3\sqrt{2}}{16} & \frac{3\sqrt{2}}{16}+\frac{3}{8} & -\frac{3}{32} & -\frac{3\sqrt{2}}{16}-\frac{3}{8} & 0 & \frac{3\sqrt{2}}{16}-\frac{3}{8} & -\frac{3}{32}\\
0 & 0 & \frac{9}{4} & -\frac{9}{4} & 0 & 0 & -\frac{9\sqrt{2}}{16} & 0 & \frac{9\sqrt{2}}{8} & \frac{9\sqrt{2}}{16} & \frac{9\sqrt{2}}{16} & \frac{27}{32} & 0 & \frac{9\sqrt{2}}{8} & 0 & -\frac{27}{32}\\
0 & 0 & \frac{3}{4} & -\frac{3}{4} & 0 & 0 & \frac{3}{4}-\frac{9\sqrt{2}}{16} & 0 & \frac{3\sqrt{2}}{8} & \frac{9\sqrt{2}}{16}-\frac{3}{4} & \frac{9\sqrt{2}}{16}+\frac{3}{4} & \frac{3}{32} & 0 & \frac{3\sqrt{2}}{8} & 0 & -\frac{3}{32}\\
0 & 0 & \frac{3}{4} & -\frac{3}{4} & 0 & 0 & -\frac{9\sqrt{2}}{16}-\frac{3}{4} & 0 & \frac{3\sqrt{2}}{8} & \frac{9\sqrt{2}}{16}+\frac{3}{4} & \frac{9\sqrt{2}}{16}-\frac{3}{4} & \frac{27}{32} & 0 & \frac{3\sqrt{2}}{8} & 0 & -\frac{27}{32}\\
0 & 0 & \frac{3}{4} & \frac{3}{4} & -\frac{3}{4} & -\frac{3}{4} & \frac{3\sqrt{2}}{16}+\frac{3}{8} & \frac{3\sqrt{2}}{16}-\frac{3}{8} & 0 & \frac{3\sqrt{2}}{16}+\frac{3}{8} & \frac{3}{8}-\frac{3\sqrt{2}}{16} & -\frac{9}{32} & \frac{3\sqrt{2}}{16}-\frac{3}{8} & 0 & -\frac{3\sqrt{2}}{16}-\frac{3}{8} & -\frac{9}{32}\\
0 & 0 & 0 & 0 & -\frac{1}{4} & \frac{1}{4} & 0 & -\frac{\sqrt{2}}{16} & -\frac{\sqrt{2}}{8} & 0 & 0 & \frac{\sqrt{2}}{32} & \frac{\sqrt{2}}{16} & \frac{\sqrt{2}}{8} & -\frac{\sqrt{2}}{16} & \frac{\sqrt{2}}{32}\\
0 & 0 & 0 & 0 & 0 & 0 & 0 & 0 & \frac{3}{4} & 0 & 0 & -\frac{3\sqrt{2}}{16} & 0 & -\frac{3}{4} & 0 & \frac{3\sqrt{2}}{16}\\
0 & 0 & 0 & 0 & \frac{9}{4} & -\frac{9}{4} & 0 & \frac{9\sqrt{2}}{16} & -\frac{9\sqrt{2}}{8} & 0 & 0 & \frac{27\sqrt{2}}{32} & -\frac{9\sqrt{2}}{16} & \frac{9\sqrt{2}}{8} & \frac{9\sqrt{2}}{16} & \frac{27\sqrt{2}}{32}\\
0 & 0 & 0 & 0 & -\frac{3}{4} & \frac{3}{4} & 0 & -\frac{9\sqrt{2}}{16}-\frac{3}{4} & \frac{3\sqrt{2}}{8} & 0 & 0 & -\frac{3\sqrt{2}}{32} & \frac{9\sqrt{2}}{16}+\frac{3}{4} & -\frac{3\sqrt{2}}{8} & \frac{3}{4}-\frac{9\sqrt{2}}{16} & -\frac{3\sqrt{2}}{32}\\
0 & 0 & 0 & 0 & \frac{3}{4} & -\frac{3}{4} & 0 & \frac{9\sqrt{2}}{16}-\frac{3}{4} & -\frac{3\sqrt{2}}{8} & 0 & 0 & \frac{27\sqrt{2}}{32} & \frac{3}{4}-\frac{9\sqrt{2}}{16} & \frac{3\sqrt{2}}{8} & \frac{9\sqrt{2}}{16}+\frac{3}{4} & \frac{27\sqrt{2}}{32}\\
0 & 0 & 0 & 0 & 0 & 0 & 0 & 0 & -\frac{3}{4} & 0 & 0 & \frac{9\sqrt{2}}{16} & 0 & \frac{3}{4} & 0 & -\frac{9\sqrt{2}}{16}
\end{pmatrix}. \tag{B6}$$

[1] S. W. Chu, S. Y. Chen, G. W. Chern, T. H. Tsai, Y. C. Chen, B. L. Lin, and C. K. Sun, Biophys. J. **86**, 3914 (2004).

[2] R. Boyd, *Nonlinear Optics*, 3rd ed. (Academic Press, Boston, 2008).

[3] R. W. Terhune, P. D. Maker, and C. M. Savage, Phys. Rev. Lett. **8**, 404 (1962).

[4] T. Y. F. Tsang, Phys. Rev. A **52**, 4116 (1995).

[5] W. A. Shurcliff, *Polarized Light: Production and Use* (Harvard University Press, Cambridge, MA, 1962).

[6] D. S. Kliger, J. W. Lewis, and C. E. Randall, *Polarized Light in Optics and Spectroscopy* (Academic Press, New York, 1990).

[7] R. M. A. Azzam and N. M. Bashara, *Ellipsometry and Polarized Light* (North-Holland, Amsterdam, 1977).

[8] M. Samim, S. Krouglov, and V. Barzda, Phys. Rev. A **93**, 013847 (2016).

[9] M. Samim, S. Krouglov, and V. Barzda, J. Opt. Soc. Am. B **32**, 451 (2015).

[10] S.-W. Chu, I. H. Chen, T.-M. Liu, P. C. Chen, C.-K. Sun, and B.-L. Lin, Opt. Lett. **26**, 1909 (2001).

[11] V. V. Yakovlev and S. V. Govorkov, Appl. Phys. Lett. **79**, 4136 (2001).

[12] D. Oron, J. Struct. Biol. **147**, 3 (2004).

[13] D. Debarre, Opt. Lett. **29**, 2881 (2004).

[14] D. Debarre, W. Supatto, A.-M. Pena, A. Fabre, T. Tordjmann, L. Combettes, M.-C. Schanne-Klein, and E. Beaurepaire, Nat. Meth. **3**, 47 (2006).

[15] S.-Y. Chen, C. Shee-Uan, W. Hai-Yin, L. Wen-Jeng, Y.-H. Liao, and C.-K. Sun, IEEE J. Select. Top. Quantum Electron. **16**, 478 (2010).

[16] L. Cui, D. Tokarz, R. Cisek, K. K. Ng, F. Wang, J. Chen, V. Barzda, and G. Zheng, Angew. Chem. **127**, 14134 (2015).

[17] D. Tokarz, R. Cisek, S. Krouglov, L. Kontenis, U. Fekl, and V. Barzda, J. Phys. Chem. B **118**, 3814 (2014).

[18] M. Born and E. Wolf, *Principles of Optics*, 7th ed. (Cambridge University Press, Cambridge, England, 1999).
[19] O. Gamel and D. F. V. James, Phys. Rev. A **86**, 033830 (2012).
[20] J. J. Gil, Eur. Phys. J.: Appl. Phys. **40**, 1 (2007).
[21] K. Kim, L. Mandel, and E. Wolf, J. Opt. Soc. Am. A **4**, 433 (1987).
[22] D. Tokarz, R. Cisek, O. El-Ansari, G. S. Espie, U. Fekl, and V. Barzda, PLoS ONE **9**, e107804 (2014).
[23] D. G. M. Anderson and R. Barakat, J. Opt. Soc. Am. A **11**, 2305 (1994).
[24] D. Layden, M. F. Wood, and I. A. Vitkin, Opt. Express **20**, 20466 (2012).
[25] M. R. Foreman, A. Favaro, and A. Aiello, Phys. Rev. Lett. **115**, 263901 (2015).
[26] D. F. V. James, P. G. Kwiat, W. J. Munro, and A. G. White, Phys. Rev. A **64**, 052312 (2001).
[27] M. S. Kaznady and D. F. V. James, Phys. Rev. A **79**, 022109 (2009).
[28] M. Samim, N. Prent, D. Dicenzo, B. Stewart, and V. Barzda, J. Biomed. Opt. **19**, 056005 (2014).
[29] A. E. Tuer, M. K. Akens, S. Krouglov, D. Sandkuijl, B. C. Wilson, C. M. Whyne, and V. Barzda, Biophys. J. **103**, 2093 (2012).
[30] This is to simplify the indices and to conform to a Stokes-Mueller notation of vector = matrix × vector. The matrices γ' can also be used directly for polarimetry, in which case there will be an additional index for the entity representing the incoming radiation as well as for the entity representing the medium.